

NBSIR 77-1396

Erosion of Brittle Materials By Solid Particle Impact

B. J. Hockey, S. M. Wiederhorn, and H. Johnson

Hockey, B. J., Wiederhorn, S. M., Johnson, H.,

Erosion of brittle materials by solid
particle impact, (Proc. 2nd Int. Symp.
Fract. Mech., State College, PA, July 26-29,
1978), Paper in Fracture Mechanics of Cera-
mics 3, R. C. Bradt, D. P. H. Hasselman,
F. F. Lange, Eds., 379-402 (Plenum Publ.
Corp., New York, NY, 1978).

New-562

NBSIR 77-1396

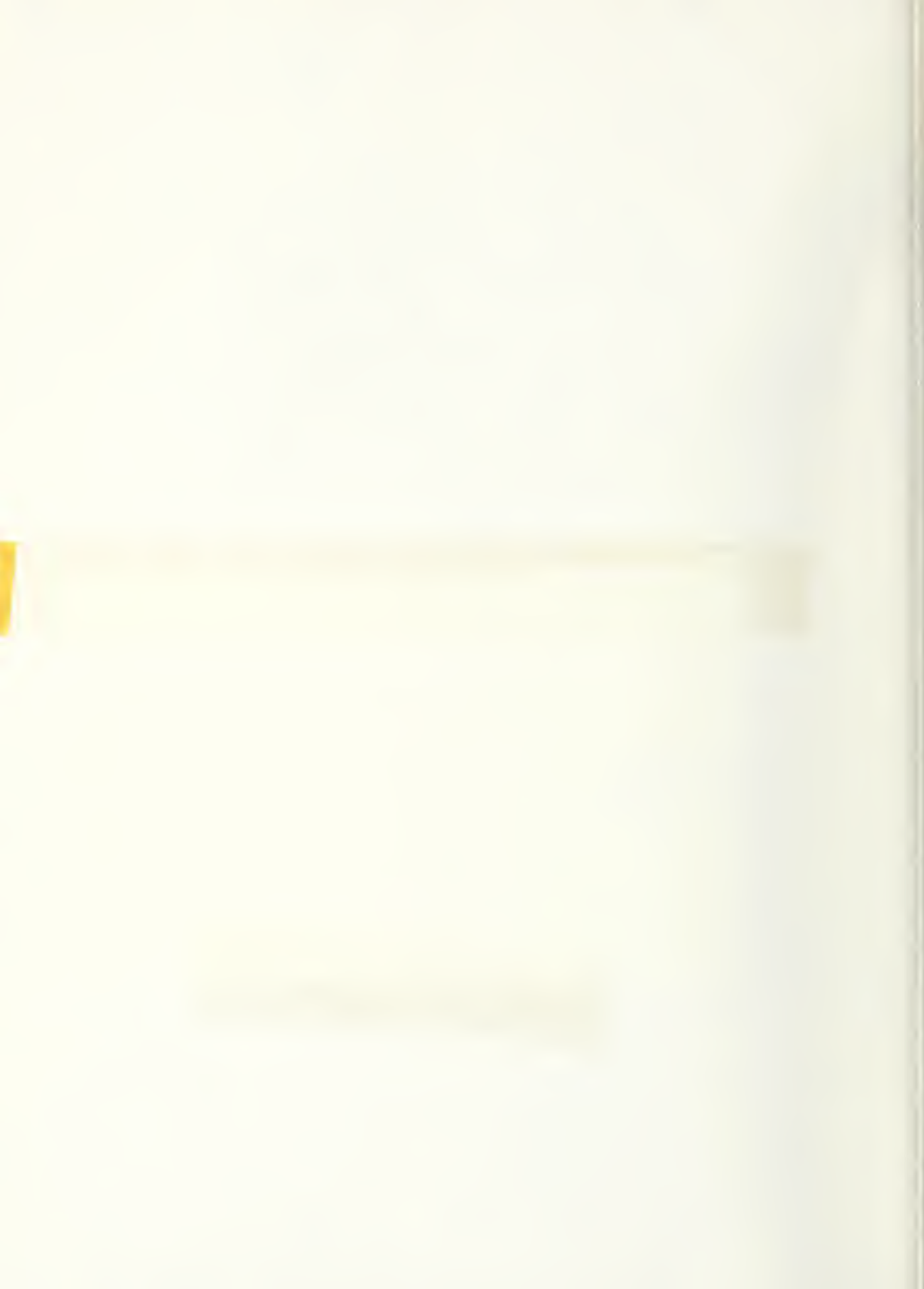
346

17904

Inorganic Ma
Institute for M
National Bure
Washington, D

Prepared for

The Pennsylvania State University
Department of Material Sciences
201 Mineral Industries Building
University Park, Pennsylvania 16802



NBSIR 77-1396

EROSION OF BRITTLE MATERIALS BY SOLID PARTICLE IMPACT

B. J. Hockey, S. M. Wiederhorn, and H. Johnson

Inorganic Materials Division
Institute for Materials Research
National Bureau of Standards
Washington, D.C. 20234

Prepared for
The Pennsylvania State University
Department of Material Sciences
201 Mineral Industries Building
University Park, Pennsylvania 16802



U.S. DEPARTMENT OF COMMERCE, Juanita M. Kreps, *Secretary*

Dr. Sidney Harman, *Under Secretary*

Jordan J. Baruch, *Assistant Secretary for Science and Technology*

NATIONAL BUREAU OF STANDARDS, Ernest Ambler, *Acting Director*

MEMORANDUM

TO : [Illegible]

FROM : [Illegible]

SUBJECT : [Illegible]

[Illegible text]

EROSION OF BRITTLE MATERIALS BY SOLID PARTICLE IMPACT

B. J. Hockey, S. M. Wiederhorn, and H. Johnson

Institute for Materials Research
National Bureau of Standards
Washington, D. C. 20234

ABSTRACT

Results are presented which show, that in addition to fracture, plastic deformation occurs and plays an important role in the erosion of brittle materials by solid particle impact. These conclusions are supported by transmission electron microscopy studies of impact damage produced in a wide variety of brittle materials and by erosive wear studies on silicon nitride and alumina. The erosive wear studies also indicate that while erosion resistance is primarily determined by fracture toughness and hardness, the relative importance of these materials parameters depends on the test conditions (e.g. temperature and angle of particle impingement).

1. INTRODUCTION

Because most ceramics are inherently brittle, they are susceptible to localized surface cracking in solid particle impact situations. Cracks formed in strong ceramics by a single impact event cause serious strength degradation for modest impact velocities (1). Moreover, continual, multiple impacts result in appreciable material loss by erosive wear. Thus, the damage resulting from solid particle impact leads to a deterioration in performance, and even failure of vital ceramic components. Despite these practical consequences, very few comprehensive erosive wear studies have been made on brittle materials. More importantly, the actual mechanisms that govern the erosive wear process in brittle materials are not well understood.

Attempts to describe the erosive wear behavior of brittle materials have tended to be semi-empirical. Nevertheless, considerable insight into this problem has been made by a recognition of

the similarity between quasi-static indentation and dynamic particle impact in the region of subsonic impact velocities. In this approach, one draws upon the similarity between the damage produced in both types of contact and uses quasi-static indentation theory to relate the extent of damage (and thus volume of material removed) to impact parameters and material properties.

This approach was first applied to an analysis of the erosive wear of brittle materials by Sheldon and Finnie (2, see also 3), who assumed that particle-target interactions were perfectly elastic. The extent of damage or volume removed was described on the basis of a classical Hertzian analysis of fracture beneath a spherical indenter. Inherently, this elastic/brittle treatment leads to the conclusion that the erosive wear of a brittle material depends on the fracture toughness (4) and on the size and distribution of pre-existing flaws (2,3).

The general assumption made by Sheldon and Finnie, that most solid particle impact events in brittle materials can be described as purely elastic contacts can be questioned. In most practical situations, surfaces are subjected to impact by angular, irregular-angular-shaped particles. Typical contact situations, therefore, resemble quasi-static indentation with indenters of small radii of curvature (i.e. sharp indenters (4)). These indenters are known to cause plastic flow (5,6) in brittle materials. Because of this, recent treatments of elastic/plastic contacts in brittle materials have suggested the importance of the flow properties (hardness) of the material as well as fracture toughness in determining the extent of fracture and erosive wear (7,8,9).

In this paper, the essential features of the quasi-static indentation approach to impact and erosive wear are examined on the basis of results from two recent experimental studies. Accordingly, the formal structure consists of two parts. In the first part, optical and transmission electron microscopy observations are used to characterize single particle impact damage in various brittle materials. In particular, emphasis is placed on illustrating the essential role of plasticity in impact situations and on demonstrating the correlation between "sharp" particle impact and quasi-static indentation. In the second part, comparative erosive wear data for alumina and silicon nitride are used to describe the dependence of erosive wear on particle velocity, angle of impingement, and temperature. These data are then discussed in the light of the single particle damage observations, and also in terms of the relative importance of fracture toughness and hardness.

2. SINGLE PARTICLE IMPACT DAMAGE

2.1 Materials

To elucidate the basic mechanisms of erosive wear of brittle materials and to provide a clearer description of the residual damage that affects material properties, solid particle impact damage studies were made on a variety of brittle materials: silicon; germanium; magnesium oxide; aluminum oxide; silicon nitride; and silicon carbide. For the most part, these materials were selected because of their practical importance and because they represent brittle materials that differ in their atomic bonding, hardness, and fracture toughness.

2.2 Experimental Procedure

All studies were conducted using an erosion tester previously described by Wiederhorn and Roberts (10). Sample surfaces were subjected to a controlled flux of abrasive grit under fixed conditions of particle velocity, angle of impingement, and temperature (up to 1000°C). To distinguish individual particle damage events - for a given set of experimental conditions - only small quantities of abrasive grit were allowed to impinge on polished (chemically or mechanically) sections. The polished sections were then examined optically to characterize the nature and extent of surface damage. In most cases, the impacted samples were thinned and examined by transmission electron microscopy to reveal details of the subsurface damage. For these samples, the thinning procedure closely followed that used in previous indentation and mechanical abrasion studies on ceramics (5,6).

2.3 Results

2.3.1 Impact Surface Damage. Room temperature, normal-incidence impact damage studies were made using measured particle velocities (11) in the range, 30 to 100 m/sec. 100 mesh (150 micron size) silicon carbide abrasive grit was used in tests on Al_2O_3 , SiC and Si_3N_4 ; whereas 150 mesh (~70 micron size) alumina grit was used in tests on Ge, Si, and MgO*. Both types of abrasive grit were composed of irregularly-shaped, angular solid particles, Fig. 1, which according to the scheme advanced by Lawn and co-workers (1) fall into the "sharp" indenter/particle category.

*Because the prethinned (~100 to 150 micron) sections of Ge, Si and MgO necessary for subsequent TEM examination tended to shatter in tests involving the larger particles, the 150 mesh alumina grit had to be used on these specimens.



Figure 1. Scanning electron micrograph illustrating angular morphology of silicon carbide particles used in impact damage and erosive wear studies.

Because the irregular impacting particles can strike the surface in any arbitrary orientation, individual impact sites were found to differ considerably in their detailed appearance. Despite this difference, the residual impact damage was found to closely resemble that produced quasi-statically in brittle materials using "sharp" indenters. In this regard, particle impact usually resulted in the formation of a permanent surface crater (indicative of surface penetration), surrounded by a well-defined, associated crack pattern. As illustrated in Figure 2, the localized fracture patterns produced by normal-incident impact were identical in all respects to those produced by quasi-static indentation. The fracture patterns usually contained both median and lateral cracks. In all materials studied, material loss from the surface occurred as the result of the extension of the lateral cracks to form a surface chips, Figure 3. This observation clearly indicates the importance of fracture to the process of erosion in brittle materials, and therefore suggests that the fracture toughness is one of the primary material parameters to be considered in problems of erosive wear.

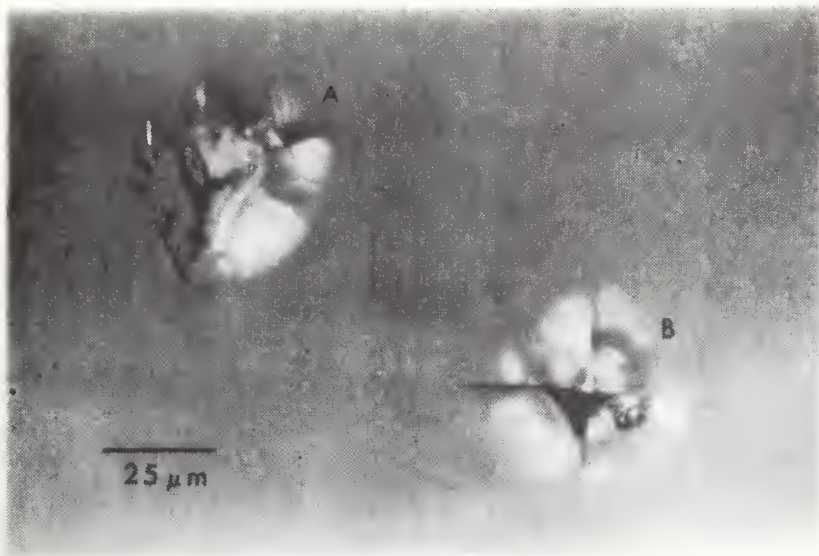


Figure 2. Comparison of surface damage produced in SiC by: (A) 90° impingement (150 micron size SiC particle at 90 m/s) and (b) quasi-static indentation (Vickers diamond pyramid, 400 gram load).

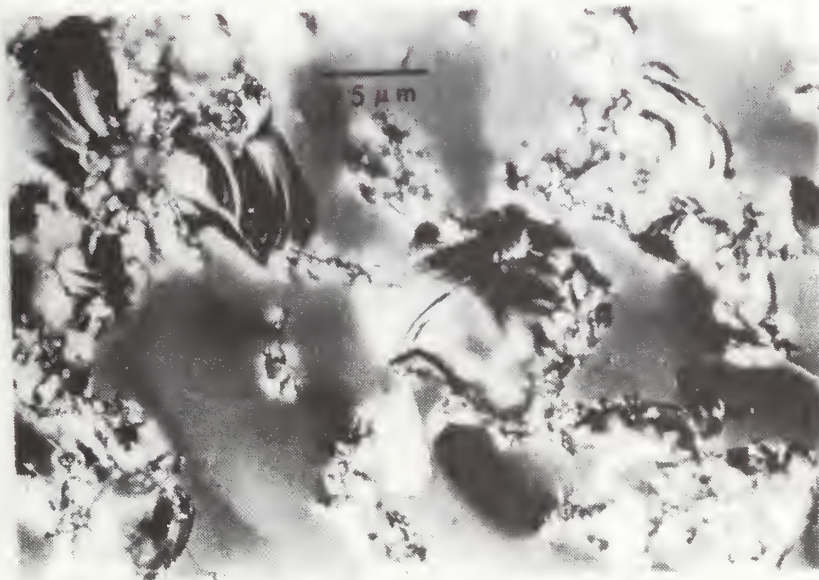


Figure 3. Surface of damage produced in Germanium by 90° impingement impact (70 micron size alumina at 90 m/s). Note material removal by the extension of lateral-vent type cracks.

2.3.2 Plastic Deformation: Occurrence and Extent. Although the materials studied in this paper are generally considered to be brittle, it can be demonstrated that plastic flow is also important to the erosive wear of these materials. As in previous studies of indentation sites in brittle materials (5,6), transmission electron microscopic examination of room temperature impact sites clearly revealed the occurrence of plastic flow by slip. This was evidenced not only by a highly deformed zone directly beneath the area of actual contact, but also by the presence of a residual dislocation pattern in the adjacent vicinity, Figures 4a and 4b. The transmission electron microscopy studies also revealed distinct differences in material response to the impacting particles. The differences appeared to be related to the nature of atomic bonding. In covalently-bonded Ge and Si, plastic deformation extended only slightly beyond the region of actual contact, Figure 4a. As a result, the radial dimension of the elastic-plastic zone in these materials was only slightly larger than the surface impression, which was small when compared to the associated fracture pattern, Figure 3. In contrast, particle impact of ionically bonded MgO resulted in extensive plastic flow. As seen in Fig. 4b, deformation extends far beyond the region of actual contact and often encompasses the associated fracture pattern.

Observations on Al_2O_3 and SiC, which possess partial ionic and covalent bonding, revealed a somewhat intermediate behavior during room temperature, normal-incidence impact. For these materials, the radial extent of the deformation was estimated to be about twice the lateral dimensions of the residual impact impression. However, under most conditions, the extent of deformation was considerably smaller than the length of the cracks.

2.3.3 Effect of Temperature. Surface damage produced in Al_2O_3 and Si_3N_4 by solid particle impact at temperatures up to $1000^\circ C$ was investigated by optical microscopy. Impact damage in Al_2O_3 was also examined by transmission electron microscopy. Over the temperature range studied, no difference was found in the general morphology of the impact fracture patterns, Figures 5a and 5b. For normal-incidence impact, localized fracture, consisting of lateral and median vent cracks, remained evident, thus indicating that material removal still occurred predominantly by surface chipping.

Transmission electron microscopy observations on Al_2O_3 , however, did reveal a considerable increase in the relative extent of the deformation associated with impact at high temperatures. In contrast to room temperature results, the radial extent of deformation by slip at 1000° was found to be comparable to the radial extent of fracture, (which appeared unchanged between 25° and $1000^\circ C$). In addition, impact at $500^\circ C$ and above resulted in a significant increase in deformational twinning. As a result, high

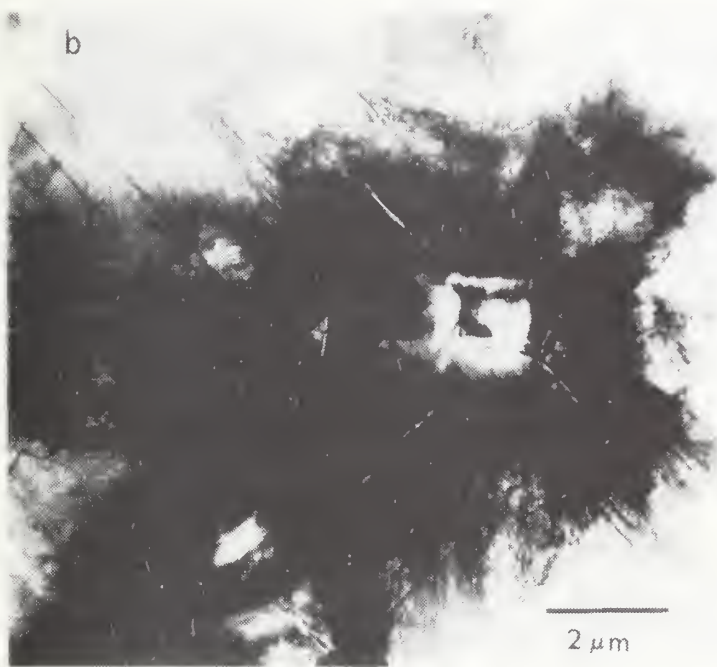
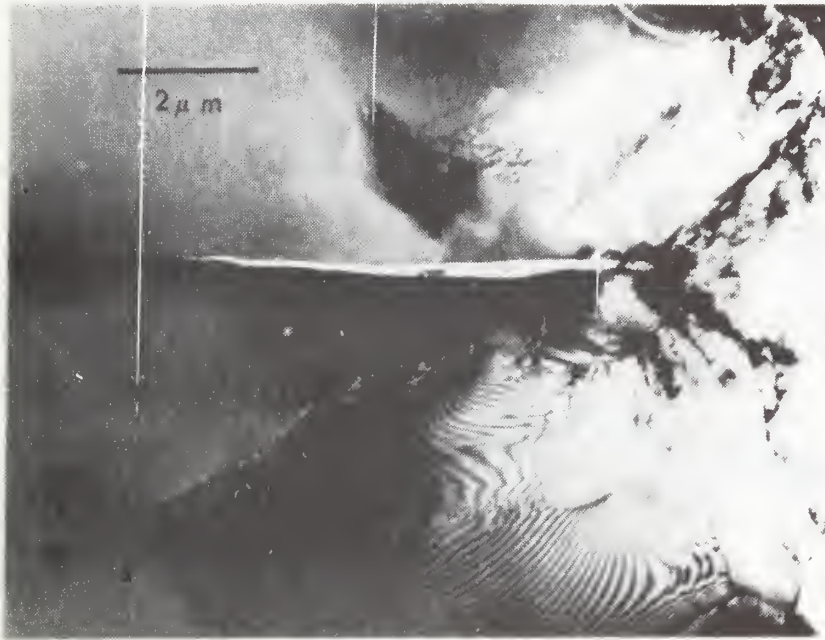


Figure 4. Transmission electron micrographs illustrating subsurface damage produced in (a) silicon and (b) MgO under similar impact conditions (90 micron size alumina particle at 90 m/s).

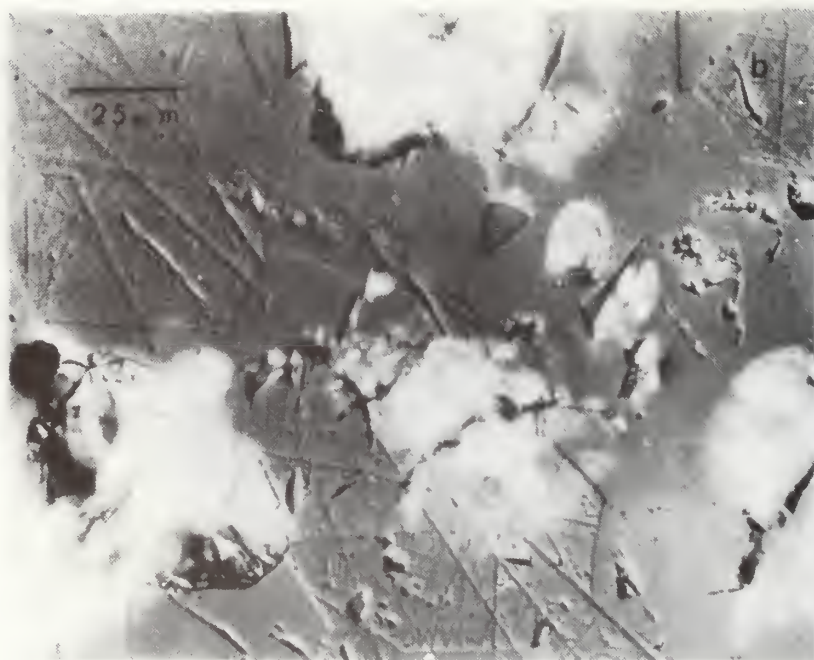
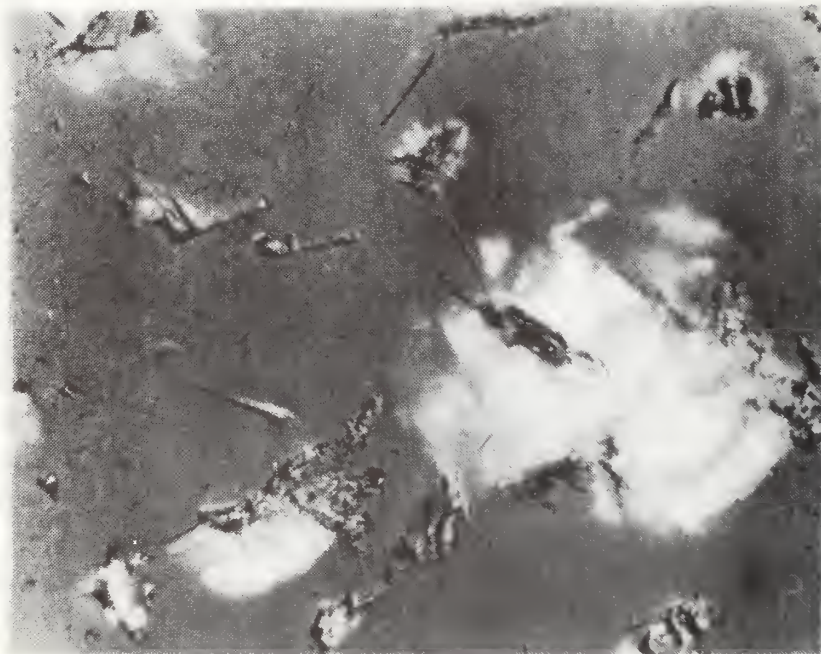


Figure 5. Normal-impingement impact damage produced in Al₂O₃ at (a) 25°C and (b) 1000°C.

temperature impact also resulted in numerous interactions between slip bands, twins, and grain-boundaries outside the region of contact.

2.3.4 Effect of Angle of Impingement. Observations on the various brittle materials included in this study showed that both the nature and extent of impact damage depends upon the angle of particle impingement. Characteristic changes that evolve as the angle of impingement is reduced to 15° are illustrated in Figures 6a and 6b. Predictably, the most obvious change is a considerable reduction in the extent of localized surface cracking. In addition, cracks produced during low angle impact were predominantly of the lateral vent type; median vent crack formation appeared to have been almost completely suppressed under these conditions.

Another characteristic of low or oblique angle impact, Figure 6a, is the formation of shallow, residual surface impressions, typically elongated along the horizontal component of particle motion. Again, transmission electron microscopy studies on SiC and Al_2O_3 confirmed that these surface impressions are the result of plastic flow, Figure 6b. Thus, oblique angle impact of the brittle materials investigated in this study is seen to result in the ploughing of material parallel to the surface. This finding suggests that at low angles of impingement plastic flow plays an important role in the erosion process and, as will be discussed, may dominate the erosion process under certain conditions (Section 4).

3.0 Erosive Wear Studies

The observations described above will now be correlated with studies of the erosive wear of hot-pressed silicon nitride and two grades of alumina (Al_2O_3) that differed microstructurally. One grade of alumina was a large-grained ($\sim 30 \mu m$), sintered product; the other was a fine-grained ($\sim 5 \mu m$), hot-pressed product. In this section, erosive wear data, describing the dependence of erosion on particle velocity, temperature, and angle of impingement are presented and compared.

3.1 Experimental Procedure

The erosive wear tests were conducted using the hot erosion tester described by Wiederhorn and Roberts (10). In this study, bulk samples (typically $1/2 \times 1/2$ in by $1/4$ in thick) were eroded by the action of 100 mesh SiC abrasive grit ($\sim 150 \mu m$ particle size), Fig. 1. Tests were conducted on each of the materials at temperatures ranging from $25^\circ C$ to $1000^\circ C$. Angles of particle impingement were varied from 15° to 90° . In all tests at oblique angles of impact, the leading edge of the test samples were protected to avoid extraneous edgewear. Rates of erosive wear were determined by measuring sample weight loss after long-term exposure.

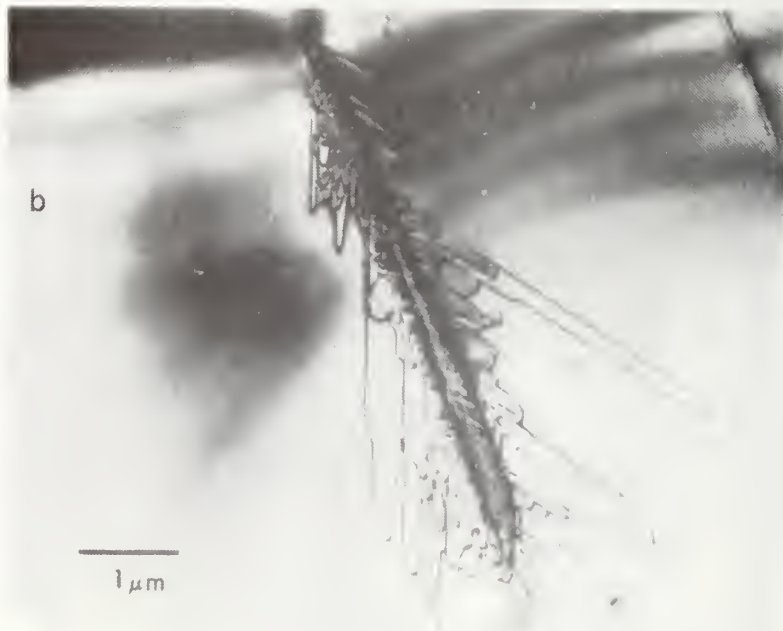
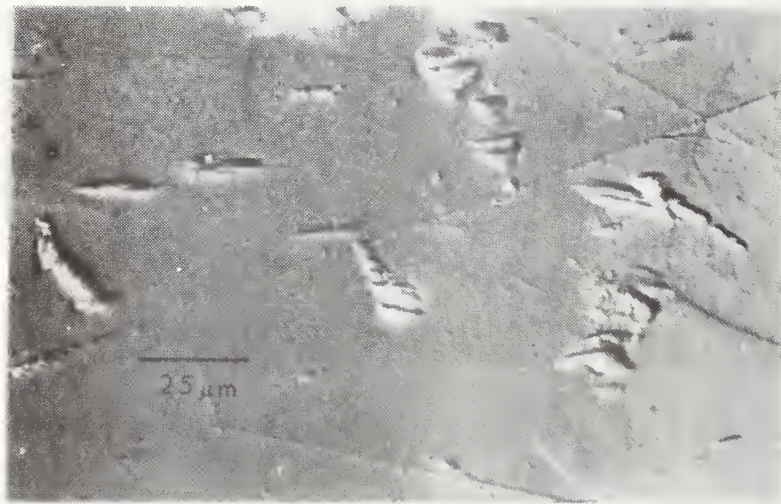


Figure 6. (a) Optical micrograph showing series of shallow surface impressions produced in Al₂O₃ by 15° impingement impact. (b) Transmission electron micrograph showing region beneath shallow surface impressions produced under similar impact conditions in SiC. Presence of dislocations emerging from contact zone and absence of cracks confirm fully plastic nature of impact event.

The erosion rates are expressed here in terms of the normalized quantity: sample weight loss per unit weight of abrasive actually striking the surface.

3.2 Results

Representative wear data, pertinent to a general description of the observed erosive wear behavior, are shown in Figures 7, 8, 9, and 10. Figures 7, 8, and 9, illustrate the dependence of erosion rate on particle velocity and temperature for the different materials. Figures 10, a and b, illustrate the dependence of erosion rate on angle of impingement at 25° and 1000°C, respectively. In each plot, the data points represent average values obtained from a minimum of three determinations; usually, however, five or more tests were made for each condition. Finally, Figures 11, a and b, illustrate the change in surface morphology that occurs when the angle of particle impingement is reduced from 90° to 15°.

3.2.1 Dependence on Particle Velocity. For all test conditions, erosive wear increases with increased particle velocity. As indicated in Figures 7 and 8, erosion rate, E , could be expressed as a simple power function of the particle velocity, V : $E \propto V^n$. On the basis of a linear least squares fit of each set of data, values of the velocity exponent, n , were found to range from 1.7 to 2.7, depending on temperature, angle of impingement, and the material tested. Although the value of n was found to increase with temperature, a consistent relationship could not be established between n and other experimental variables.

3.2.2 Temperature Dependence. A significant effect of temperature on the erosive wear of the materials studied was only apparent in the data for oblique angles of incidence (i.e. $\alpha=15^\circ$ and 30°). This is illustrated in Figure 7 and in Figure 8, where 90° and 15° impingement data for each material are compared.

As seen in Figure 7, erosive wear rates at 90° impingement are, for all practical purposes, independent of temperature between 25° and 1000°C . For each material, changes in rate of wear or slope, n , with temperature were too small to be considered statistically significant. The 90° impingement data, moreover shows that hot-pressed silicon nitride is more resistant to erosion than the hot-pressed alumina (by a factor of ~ 1.5 on a volume loss basis), which in turn, is more resistant than the sintered alumina (by a factor of $\sim 2-3$).

In contrast to the results described above, data obtained using particle impingement angles of 30° and 15° both* indicated

*For brevity, the data obtained for 30° impingement are not presented in this paper.

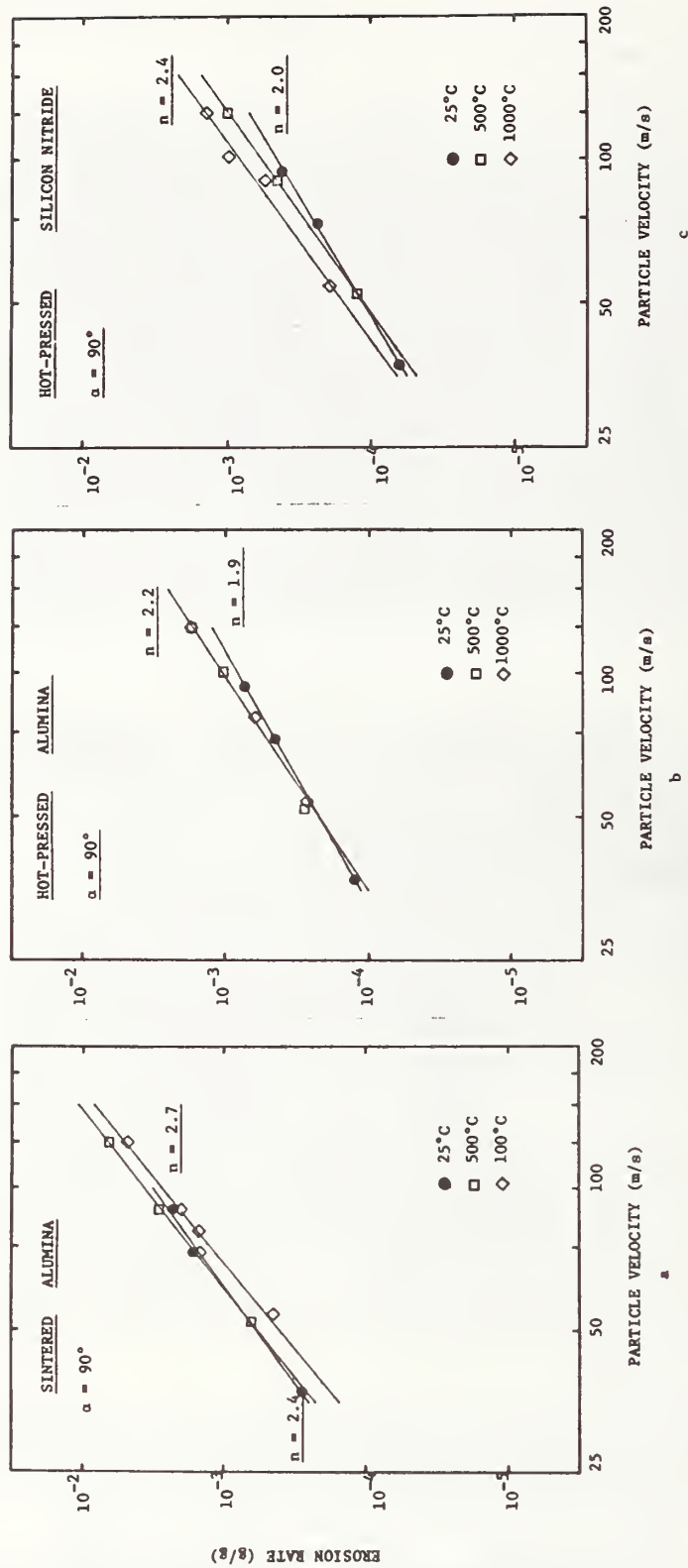


Figure 7. Erosive wear rate as a function of particle velocity and temperature for 90° impingement: (a) Sintered alumina; (b) Hot-pressed alumina; (c) Hot-pressed silicon nitride.

that erosion is affected significantly by temperature for oblique angles of impact. Under these conditions the erosive wear data for each material exhibited a substantial increase in slope, n , as the temperature was increased from 25°C to 1000°C. This increase can be seen in Figures 8a, 8b, and 8c, where 15° impingement data at 25°C and 1000°C are compared for each material. For hot-pressed silicon nitride, Figure 8a, the value of n increased from 1.7 at 25° to 2.7 at 1000°C. Although the erosion behavior of the hot-pressed alumina was similar to that of the hot-pressed silicon nitride, the increase in n from 2 to 2.6 was not as great as for the hot-pressed silicon nitride. A similar observation is made for the sintered alumina, for which n increased from 2.1 to 2.6 over the same temperature range. The erosion behavior of the sintered material, however, is seen to differ significantly from that of the hot-pressed materials, in that erosive wear rates are lower at 1000°C than at 25°C over most of the range of particle velocities used in these tests (Figure 8c).

The net effect of temperature on erosion wear at oblique angles of impingement is illustrated in Figure 9 for the 15° data. At 25°C, Figure 9a, hot-pressed silicon nitride exhibits better erosion resistance than the two types of alumina, while the hot-pressed alumina exhibits better erosion resistance than the sintered alumina. At both 15° and 30° impingement, the room temperature erosion behavior of the materials was comparable to that found at 90° impingement. In contrast to these results at 25°C, results obtained at 1000°C for both 30° and 15° impingement, Figure 9b, show little difference in the erosive wear of these materials. Thus at 1000°C, the erosion behavior at oblique angles of impingement differs significantly from that found at $\alpha=90^\circ$. This change in erosive behavior at high temperatures and oblique angles of impingement appears to be related to an increase in the role of plastic flow in the erosion process (see Sections 3.2.3 and 4.0).

3.2.3 Dependence on Angle of Impingement. Measurements of the effect of impingement angle on the erosion rate were also made to investigate mechanisms of erosion. Past studies (12,13) have shown that erosion by a brittle mode is characterized by a maximum in erosion rate at 90° impingement and by a relatively rapid decrease in erosion rate as the impingement angle is decreased. Ductile erosion, by contrast, is characterized by a peak in the erosion rate at an angle of impingement of ~15-20° with a decrease in the erosion rate at higher and lower angles of impingement. It is generally recognized that most metals undergo combined modes of erosion. In the present investigation, the observed variation in rate of erosion with impingement angle for each material also indicates a combined mode of erosion.

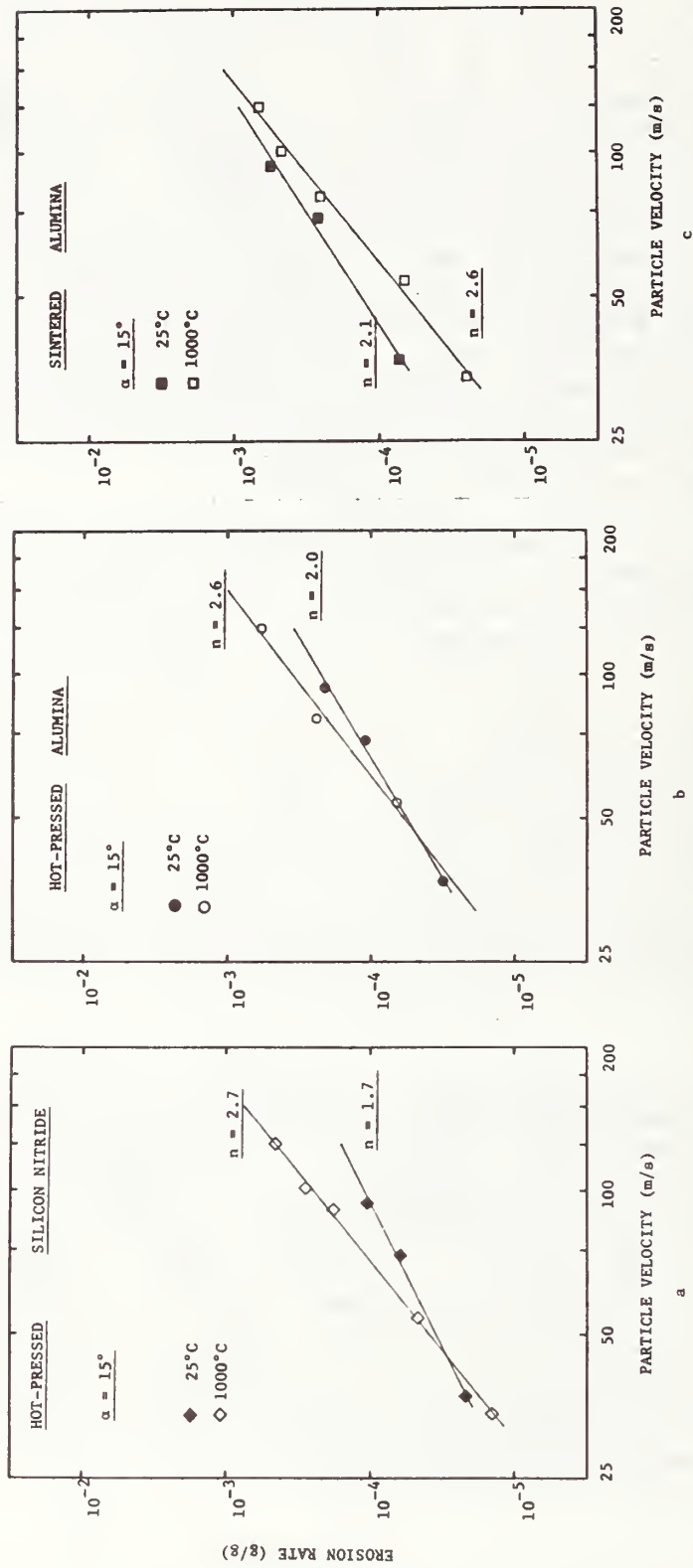


Figure 8. Erosive wear rate as a function of particle velocity for 15° impingement at 25° and at 1000°C: (a) hot-pressed silicon nitride; (b) hot-pressed alumina; (c) sintered alumina.

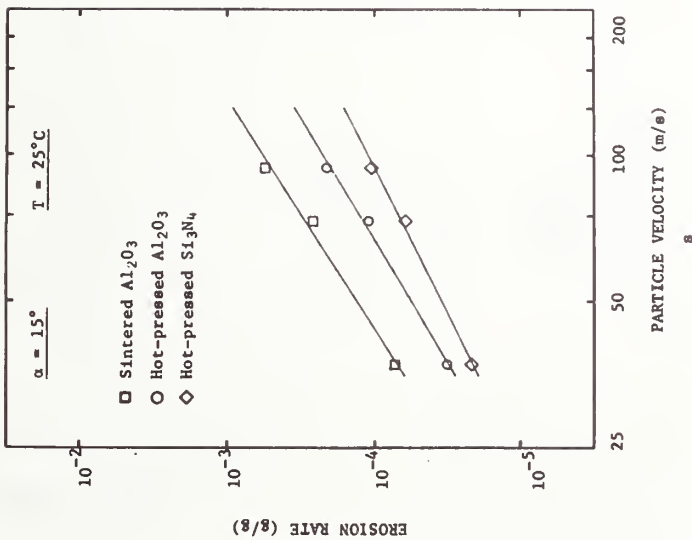
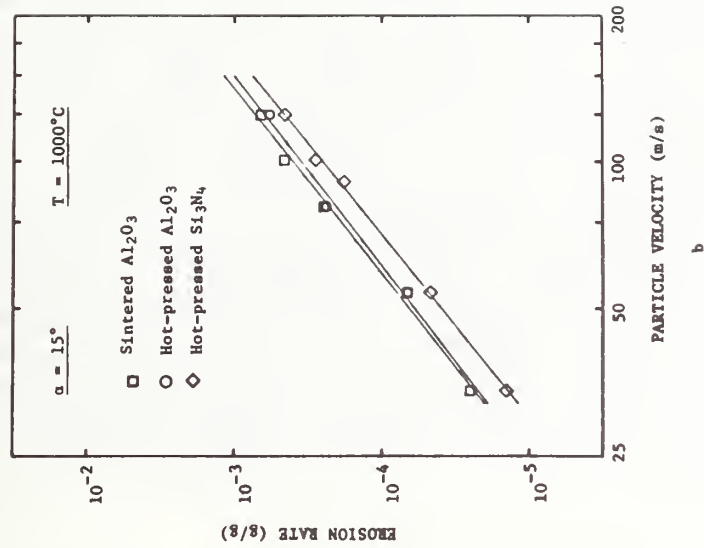


Figure 9. 15° impingement erosive wear data for hot-pressed silicon nitride, hot-pressed alumina, and sintered alumina compared at: (a) 25°C and (b) 1000°C.

In Figures 10a and b, erosive wear rates for silicon nitride are plotted as a function of impingement angle for temperatures of 25°C and 1000°C respectively. For both temperatures, the data are compared with a theoretical treatment of brittle erosion that will be discussed below (Section 4). As can be seen in Figure 10a, erosion rate follows the theoretical curve for angles as low as 30°. However, at 15° impingement, the rate of erosion is approximately 5 times that predicted by theory. At 1000°C, Figure 10b, this same type of comparison also indicates a large difference between measured and predicted erosion rate but now this difference is observed over a wider range of impingement angles. At 15°, the measured erosion rate is approximately 7 times the predicted rate, while at 30° impingement the measured erosion rate is approximately 2 times the predicted rate. At 45° impingement, the measured erosion rate is still 1.6 times the predicted rate. Similar differences between measured and predicted wear were also found in the data for both types of alumina. These deviations between measured and predicted behavior suggest that wear of the materials studied occurs by a mixed mode of erosion, with the ductile mode becoming important at low angles of impingement. On this basis,

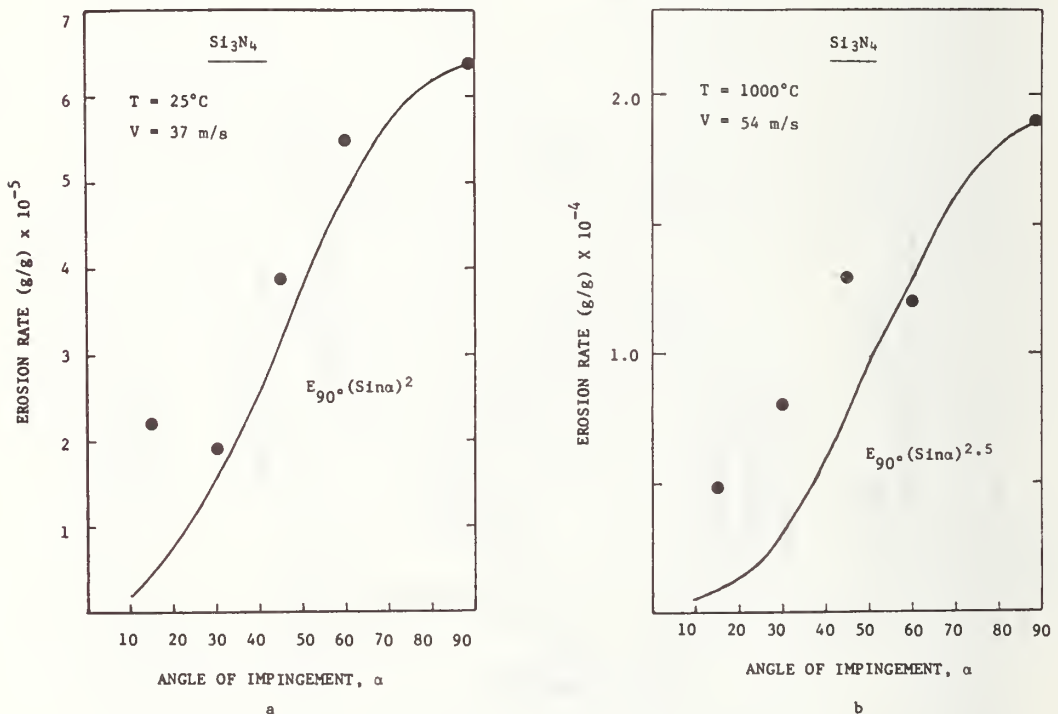


Figure 10. Erosive wear rate of hot-pressed silicon nitride plotted as a function of angle of particle impingement α . Full-line curves represent predicted dependence for purely brittle behavior (see text).

the data also indicates that as the temperature is increased, the role of plastic flow becomes increasingly more important in the erosion process.

The above conclusions are supported by optical and scanning electron microscopy studies of the erosion surfaces. Under erosion conditions where there is good agreement between measured and predicted wear, (i.e. $\alpha = 90^\circ$ to 30° at 25°C , and $\alpha = 90^\circ$ to $\sim 45^\circ$ at 1000°C , Figure 10) the resultant surfaces are similar and clearly indicate that material has been removed primarily by a brittle chipping process, Figure 11a. By contrast, erosive wear at lower angles of impingement (i.e. $\alpha = 15^\circ$ at 25°C and $\alpha = 15^\circ$ and 30° at 1000°C), results in relatively smooth surfaces, Figure 11b. These surfaces, moreover, are characterized by numerous smooth furrows or wear scars indicative of material removal by a ductile ploughing process. While lateral venting is also observed along the edges of the wear scars, and obviously contributes to material removal, it is nevertheless clear that, for these conditions, the mechanism of erosion more closely resembles the ductile mode of wear, normally attributed only to metals. These observations, moreover, are consistent with the single particle impact damage results discussed in Section 2.

4. DISCUSSION

The results presented in this paper all point to the importance of plastic deformation in the erosion of materials that otherwise exhibit brittle behavior. Plastic flow appears to enter the erosion process in two distinct ways: by subsurface deformation that enhances surface chipping; and by shear deformation wherein fracture is minimal and material is removed primarily by a plastic cutting process.

In the chipping mode of erosion, material removal occurs primarily by the extension of lateral vent type cracks (as in Figure 3). The nature of these cracks and the way in which they grow during quasi-static indentation has been described by Lawn and Swain (14) for glass, and by Hockey and Lawn (6) and Evans and Wilshaw (7) for crystalline materials. These studies have shown that lateral vent cracks are peculiar to "sharp indenter" contact situations and that they fully develop only after removal of the applied load. Previous studies by transmission electron microscopy (5,6) have shown that the indentation of brittle materials (e.g. Al_2O_3 and SiC) also results in intense deformation, which is generally constrained within the region of contact. As a consequence, large residual stresses are produced. These stresses are believed to provide the driving force for lateral-vent crack formation. Based on results obtained in the present study, a similar explanation is advanced for the formation of lateral vent cracks during solid particle impact events. Accordingly, the

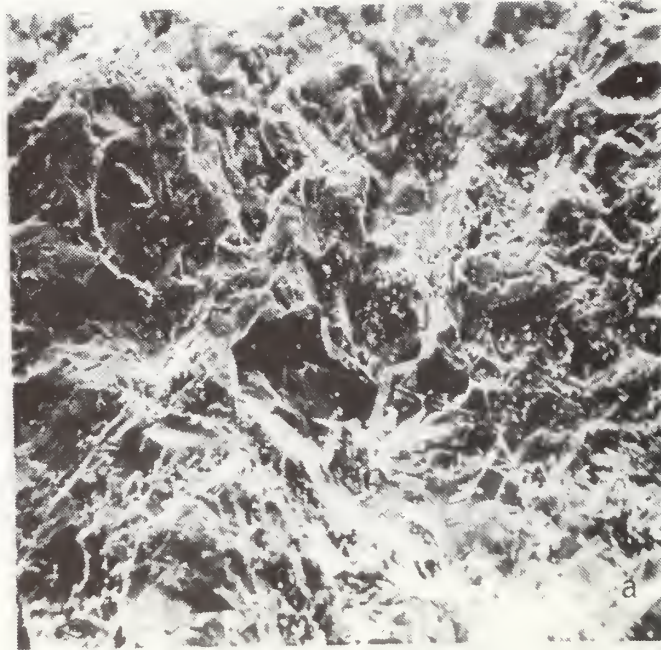


Figure 11. Scanning electron micrographs showing surface morphology of sintered alumina test samples after erosion at 1000°C: (a) 90° impingement angle and (b) 15° impingement angle.

erosion of brittle materials by surface chipping should depend both on resistance to crack extension (fracture toughness) and on resistance to plastic flow (hardness).

Recently, Evans et al.(8,9) have presented a theoretical treatment for the erosion of brittle materials by "sharp" particle impact. They estimate the erosion rate from the depth of penetration of the incoming particle and the size of the lateral cracks that form during the impact event. Accordingly, this treatment incorporates both the hardness, H , and the critical stress intensity factor, K_C , in the equation that describes the amount of material removed per impact \bar{v}_i :

$$\bar{v}_i \approx V_0^{2.5} R_p^4 \rho_p^{0.3} H^{-0.3} K_C^{-1.5} \quad (1)$$

where V_0 is the incoming particle velocity; R_p is the particle radius; ρ_p is the particle density. The exponents in this equation are obtained in part through a mathematical analysis of the impact problem, and in part through an experimental investigation of the extent of damage that occurs in materials during impact. In applying this expression to multiple impact situations, it is assumed that interactions between adjacent impacts are negligible and that each impact event is similar. The theory is the first to describe the erosion of brittle materials in terms of an elastic-plastic phenomenon and provides a good basis for discussing the erosion data presented in this paper.

Several aspects of the data in this paper can be described in terms of the theory developed by Evans and his colleagues. First and foremost, the theory assumes that plastic flow occurs in the region beneath the contact area. The results of Section 2, provide direct evidence to support this assumption. Furthermore, as discussed earlier in this Section, the formation of lateral vent cracks appears to be directly related to the occurrence of plastic deformation and the development of large residual stresses.

A second experimental parameter that can be compared with the theory developed by Evans et al. is the exponent of the impact particle velocity. In the present study, velocity exponents ranging from 1.7 to 2.7 were obtained; the lower values being representative of room temperature data at low impingement angles, the high values being representative of the high temperature data. The theory developed by Evans et al. predicts an exponent of 2.5, which differs slightly but significantly from the values obtained in this study. The difference between the predicted and experimental values of the velocity exponent can be traced to the assumption used to predict the amount of material removed during multiple impacts. The erosion rate per particle impacting the surface was assumed to be proportional to the depth of the plastic zone and

the square of the size of the lateral cracks. Minor variations in this assumed proportionality with velocity would lead to a velocity exponent that differed from the one given by Evans et al. Thus, a dependence on velocity of lateral crack shape or the depth from which the cracks originate could significantly alter the value of the velocity exponent. Furthermore, the theory assumes that all particles hitting the surface cause the same amount and type of damage. Because of a spread in the velocity of particles in an erosion experiment, the arbitrary orientation of particles as they contact the surface, and the surface roughness that develops during the erosion process, this assumption can not be satisfied rigorously. As a consequence, the velocity exponent might be expected to differ from the value of 2.5 predicted from the theory. Considering the difficulty of incorporating these various parameters into the theory, modification of the theory to handle these parameters may not be possible.

A final comparison between theory and experiment can be made by considering the relative erosion rates of alumina and silicon nitride at normal angles of impact. Based on volume loss, the erosion rate of the sintered aluminum oxide is approximately four times that of the silicon nitride at 25°C. Since the room temperature hardness of these two materials are about the same relative differences in the erosive wear of the two materials should depend only on the critical stress intensity factors of the two materials. Specifically, the ratio of erosion rates should be given by ratio of the two K_c values raised to the 1.5 power, i.e.,

$$\bar{v}_i(\text{Al}_2\text{O}_3)/\bar{v}_i(\text{Si}_3\text{N}_4) \propto [K_c(\text{Al}_2\text{O}_3)/K_c(\text{Si}_3\text{N}_4)]^{1.5} \quad (2)$$

Given that K_c for Al_2O_3 is $2.5 \text{ MN/m}^{3/2}$ (15) and K_c for Si_3N_4 is $5 \text{ MN/m}^{3/2}$ (16), the predicted ratio of erosion wear is $\sim 2.9^*$. Considering the approximations involved in the theory, and the uncertainties of the experimental values of K_c , the predicted ratio is considered to be in good agreement with the experimental value. As predicted by the theory, normal-impingement erosion seems to be controlled by the resistance of the material to crack propagation.

A similar prediction of the erosion rate can be made from the high temperature erosion data. However, since the hardness of

*Because $30 \mu\text{m}$ grain Al_2O_3 was used in these studies, the contact area during impact was usually confined to a single grain. Therefore, single crystal values of K_c were used in this comparison.

Si₃N₄ has not been measured at elevated temperatures, the prediction must be considered more approximate than the room temperature prediction. Assuming the hardness of aluminum oxide and silicon nitride are equal at 1000°C, and using measured values of the critical stress intensity factors for the two materials (~ 1.8 MN/m^{3/2} for single crystal Al₂O₃ at 800°C; ~ 5 MN/m^{3/2} for Si₃N₄ at 1000°C), the erosion rate of the aluminum oxide is expected to be ~ 4.6 times the erosion rate of silicon nitride. The ratio, ~ 3 , of the two erosion rates obtained experimentally is in qualitative agreement with the predicted value.

A similar qualitative comparison of data between the hot-pressed aluminum oxide and the other two materials cannot be made because the critical stress intensity factor for this material was not measured. However, because of the small grain size of hot-pressed aluminum oxide, a polycrystalline value of K_{IC} would have to be used to describe the erosion rate. Since polycrystalline values of K_{IC} are typically higher than single crystal values, the erosive wear of the hot-pressed aluminum oxide would be expected to be less than that of the sintered aluminum oxide. This expectation is confirmed by experimental observation.

Considering all of the data presented in this paper on erosion at normal incidence of impact, the elastic/plastic treatment developed by Evans et al.(8) seems to provide a good semi-quantitative description of the erosion process. Plastic flow is always observed beneath the contact area; the dependence of erosion rate on particle velocity agrees qualitatively with the predicted dependence; and the relative erosion resistance of the three materials studied is roughly that expected from the theory. However, consideration of the observed variation in erosive wear with impingement angle indicates other factors influence the erosion process. By modifying the theory presented by Evans et al. to include oblique angles of impact, it can be shown that erosion at low angles of impact involves shear deformation as well as brittle fracture.

Although the theory of Evans et al. was developed for normal particle incidence, it can be extended to oblique angles of incidence by assuming that lateral crack extension and penetration is determined only by the normal component of the particle velocity. Based on this assumption, the erosion equation of Evans et al. is modified by substituting the normal component for the particle velocity, $V_0 \sin \alpha$, into equation 1. Thus, the dependence of erosion rate on angle of impingement should be given by:

$$\bar{v}_i \propto (V_0 \sin \alpha)^n, \quad (3)$$

where V_0 is the particle velocity, α is the angle of impingement, and where the experimental velocity exponent, n , has been substituted for the value of 2.5 given in equation 1.

Equation 3 is compared in Figures 10a and b with erosion data for hot-pressed Si_3N_4 . At 25°C , n was found to have a value of ~ 2 for normal-impingement erosion. The data is, therefore compared with a plot of the rate of erosion for normal impact times $\sin^2\alpha$ in Figure 10a. The comparison of the theoretical and experimental values of the erosion rate is satisfactory for impingement angles greater than 30° . However at 15° impingement, the measured rate of erosion is approximately five times the predicted value. A similar comparison of experimental with predicted erosion rates is given in Figure 10b, for data obtained on hot-pressed silicon nitride at 1000°C . At this temperature, the value of n obtained for normal impact was ~ 2.5 . A plot of $\sin^{2.5}\alpha$ times the erosion rate for normal impact is found to agree with the experimental data only for 60° impact. At lower impact angles, the erosion rate is larger than expected.

The deviation of experiment from theory described above can be attributed to the increased importance of a shear mechanism of erosion at low impact angles. Particles impacting upon the target surface remove material primarily by ploughing in a manner described in much of the erosion literature on metals. In view of the microscopic evidence for plastic flow underneath the impact sites, it is reasonable to suggest that the mechanism of material removal in the plowed area is by ductile flow. However considering the fact that some lateral venting also occurs, a contribution of fracture to erosion at oblique angles cannot be dismissed. If plastic ploughing is the primary mechanism of erosion, then the erosion rate should depend more on the resistance to deformation (i.e. hardness), than on fracture toughness. Therefore, materials that have the same hardness, but different fracture toughness are expected to have the same erosion rate for similar erosion conditions. This conclusion is supported by the results shown in Figure 9b, which compares the 15° impingement data obtained at 1000°C . Little difference is seen between the data for the three materials. Had the erosion data been presented in terms of the volume loss rather than the weight lost per weight of impacting particles, the comparison would have been even closer. In contrast, distinct differences in the room temperature erosion behavior for oblique angles of impact, Figure 9a, suggests that at room temperature fracture still plays a role in the erosion process.

5. SUMMARY

In this paper, results are presented which show that plastic flow plays an important role in the erosion of brittle materials.

At high impact angles, the occurrence of plastic flow provides an explanation for the growth of cracks that result in material removal from the target surface. At oblique angles of impingement, impact damage is often free of cracks suggesting that material removal occurs by a shear deformation process. Erosive wear data obtained in this study further support the importance of plastic deformation to the erosion process. The experimental data presented in this paper also provides support for the elastic-plastic erosion theory proposed recently by Evans et al. (8), which describes material removal in terms of the penetration and extension of lateral vent-type cracks. At oblique angles of impingement, however, material removal also occurs by a shear deformation process of the type usually used to describe the erosion of metals. By increasing the target temperature from 25°C to 1000°C, deformation of the target materials during impact is enhanced, and material removal by shear deformation occurs at higher impact angles. Since both brittle and ductile modes of material removal occur, erosive wear is determined by both hardness and fracture toughness.

Acknowledgement

The authors wish to acknowledge the support of the Office of Naval Research.

REFERENCES

1. Lawn, B. R., and Marshall, D. B., this volume.
2. Sheldon, G. L., and Finnie, I., Trans. ASME 88B, 393 (1966).
3. Oh, H. L., Oh, K. P. L., Vaidyanathan, S., and Finnie, I., "The Science of Ceramic Machining and Surface Finishing". NBS Special Publication 348, edited by S. J. Schneider and R. W. Rice, p. 119 (1972).
4. Lawn, B. R., and Wilshaw, T. R., J. Mater. Sci. 10, 1049 (1975).
5. Hockey, B. J., J. Amer. Ceram. Soc., 54, 223 (1971).
6. Hockey, B. J., and Lawn, B. R., J. Mater. Sci., 10, 1275 (1975).
7. Evans, A. G., and Wilshaw, T. R., Acta Met. 24, 939 (1976).
8. Evans, A. G., Gulden, M.E., Rosenblatt, M.; to be published in Proc. Roy. Soc.
9. Evans, A. G., this volume.

10. Wiederhorn, S. M., and Roberts, D. E., Bull. Am. Ceram. Soc. 55, 185 (1976).
11. Ruff, A. W., and Ives, L. K. Wear, 35, 195 (1975).
12. Sheldon, G. L., and Finnie, I., Trans. ASME 89B, 387 (1966).
13. Sheldon, G. L., Trans. ASME 92D, 619 (1970).
14. Lawn, B. R., and Swain, M. V., J. Mater. Sci. 10, 113 (1975).
15. Wiederhorn, S. M., Hockey, B. J., and Roberts, D. E., Phil. mag. 28, 783 (1973).
16. Evans, A. G., and Wiederhorn, S. M., J. Mater. Sci. 9, 276 (1974).

U.S. DEPT. OF COMM. BIBLIOGRAPHIC DATA SHEET	1. PUBLICATION OR REPORT NO. 77-1396	2. Gov't Accession No.	3. Recipient's Accession No.
--	---	---------------------------	------------------------------

1. TITLE AND SUBTITLE Erosion of Brittle Materials by Solid Particle Impact	5. Publication Date
	6. Performing Organization Code

7. AUTHOR(S) B. J. Hockey, S. M. Wiederhorn, and H. Johnson	8. Performing Organ. Report No.
--	---------------------------------

9. PERFORMING ORGANIZATION NAME AND ADDRESS NATIONAL BUREAU OF STANDARDS DEPARTMENT OF COMMERCE WASHINGTON, D.C. 20234	10. Project/Task/Work Unit No. 3130150
	11. Contract/Grant No.

12. Sponsoring Organization Name and Complete Address (Street, City, State, ZIP) The Pennsylvania State University Department of Material Sciences 201 Mineral Industries Building University Park, Pennsylvania 16802	13. Type of Report & Period Covered
	14. Sponsoring Agency Code

15. SUPPLEMENTARY NOTES

16. ABSTRACT (A 200-word or less factual summary of most significant information. If document includes a significant bibliography or literature survey, mention it here.)

Results are presented which show, that in addition to fracture, plastic deformation occurs and plays an important role in the erosion of brittle materials by solid particle impact. These conclusions are supported by transmission electron microscopy studies of impact damage produced in a wide variety of brittle materials and by erosive wear studies on silicon nitride and alumina. The erosive wear studies also indicate that while erosion resistance is primarily determined by fracture toughness and hardness, the relative importance of these materials parameters depends on the test conditions (e.g. temperature and angle of particle impingement).

17. KEY WORDS (six to twelve entries; alphabetical order; capitalize only the first letter of the first key word unless a proper name; separated by semicolons)

Ceramics; erosion; fracture; plastic flow; solid particle impact; transmission electron microscopy.

18. AVAILABILITY	19. SECURITY CLASS (THIS REPORT)	21. NO. OF PAGES
<input checked="" type="checkbox"/> Unlimited	UNCLASSIFIED	26
<input type="checkbox"/> For Official Distribution. Do Not Release to NTIS	20. SECURITY CLASS (THIS PAGE)	22. Price
<input type="checkbox"/> Order From Sup. of Doc., U.S. Government Printing Office Washington, D.C. 20402, SD Cat. No. C13	UNCLASSIFIED	\$4.50
<input checked="" type="checkbox"/> Order From National Technical Information Service (NTIS) Springfield, Virginia 22151		

